Supercond. Sci. Technol. **23** (2010) 025002 (6pp) doi:10.1088/0953-2048/23/2/025002

The field, temperature and strain dependence of the critical current density of a powder-in-tube Nb_3Sn superconducting strand

Xi Feng Lu[1] **and Damian P Hampshire**

Superconductivity Group, Department of Physics, Durham University, Durham DH1 3LE, UK

E-mail: xifeng.lu@nist.gov and d.p.hampshire@durham.ac.uk

Received 29 September 2009, in final form 13 October 2009
Published 10 December 2009
Online at stacks.iop.org/SUST/23/025002

Abstract

We present critical current density (J_C) data as a function of magnetic field, temperature ($4.2\ K \leqslant T \leqslant 14\ K$) and intrinsic strain ($\varepsilon_I$) for a high performance powder-in-tube (PIT) Nb_3Sn strand. Although the critical current density is very high, it is demonstrated that there is no stronger strain sensitivity than for Nb_3Sn strands of other types and that the reversible strain window encompasses at least $-0.60\% < \varepsilon_I < 0.25\%$. The n-value of the PIT Nb_3Sn strand, derived from the electric field–current density (E–J) characteristics, is two or three times larger than those of strands made using other production processes. However, the normalized n-index as a function of intrinsic strain still shows a similar behaviour to those for other strands. The relation between the n-index and the critical current is described by the empirical power law of the form $n = 1 + rI_C^s$, where r and s are approximately 3 and 0.5 respectively. We conclude that the increase in J_C and the n-value for PIT strands is achieved while maintaining good tolerance to strain.

1. Introduction

Although Nb_3Sn was discovered 50 years ago, the International Thermonuclear Experimental Reactor (ITER) [1–4] has in the last 10 years driven the continuous development of better Nb_3Sn strands for high magnetic field applications. In parallel, high field projects for the high energy Physics community including the 1 GHz NMR [5], and the Next European Dipole (NED) programme [6] launched in 2004 (requiring non-Cu $J_C > 1500\ A\ mm^{-2}$ at 4.2 K and 15 T) [7], have encouraged the development of strands with higher critical current density in high magnetic fields. At present bronze-route and advanced internal-tin Nb_3Sn strands have sufficiently low ac losses for fusion (ITER) applications but the engineering J_C (defined as the critical current divided by the total cross-section area of the strand) in these strands is also low, typically 300–600 A mm^{-2} at 4.2 K and 12 T (non-Cu $J_C \sim$ 800–1200 A mm^{-2}) [1]. For high field applications where ac losses are less important, the restacked-rod-process (RRP) internal-tin Nb_3Sn strands and powder-in-tube (PIT) Nb_3Sn strands are relevant because these strands carry very high non-Cu J_C (4.2 K, 12 T) values of ~2500–3000 A mm^{-2} [1, 8–10]. In figure 1, J_C as a function of field at 4.2 K [8, 11–13] is shown for these four main types of strands—including the high J_C PIT strand that is the subject of this paper. The data show that the magnitude of J_C in the RRP and PIT strands lies far above other two types.

In addition to high J_C, the PIT strand route offers other very attractive properties: the non-Cu J_C has been continuously increased to ~2700 A mm^{-2} (4.2 K, 12 T) [14, 15] while maintaining inherently decoupled filaments with low effective filament diameters (which can be similar to the physical dimensions of the filaments themselves [9]); the V–I transitions are very sharp, characterized by the extremely high n-index (2–3 times of that of other strands) confirmed in this paper; the PIT strand can achieve high J_C with relatively short heat-treatment times (only ~20–50 h). In addition to the technological importance of PIT strands, the good compositional homogeneity and uniform and fine grain size of the microstructure [16, 17, 14] means that these materials are excellent candidates for flux pinning studies

[1] Present address: NIST, Boulder, USA.

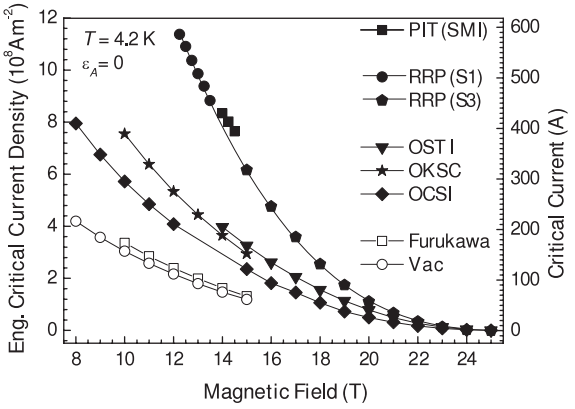

Figure 1. Engineering critical current density J_C (and critical current I_C) versus magnetic field for 0.81 mm diameter Nb_3Sn strands made by different manufacturers. The Vac and Furukawa are bronze-route strands [27]. OCSI, OKSC, and OST I are advanced internal-tin strands [39]. Samples S1 and S3 are the RRP strands [13]. The PIT (SMI) sample is the powder-in-tube strand.

that can address the long-standing issue of how to increase J_C further towards the theoretical depairing current density which in high fields is still at least 2 orders of magnitude higher than anything achieved in any technological strands [18]. On the other hand, PIT strands are relatively expensive. Although PIT processing of Nb_3Sn has been aided by the progress with HTS [19, 20] and MgB_2 [21] PIT superconductors, it is still relatively complex and needs further refinement to reduce the amount of expensive unreacted Nb that remains after the heat-treatment and to increase the A-15 fraction in the non-Cu area [10]. New tubular approaches are being attempted which may simplify the production process [22] and may yet make these materials more commercially viable.

It is well known that the large unavoidable stresses (and strains) produced during the process of cool-down and operation of high field magnets mean that the brittle properties and strain tolerance of the superconducting properties of the Nb_3Sn are important [2–4, 23]. Furthermore, after the strain behaviour of RRP strands was found to be significantly different to bronze-route strands it opened the question of whether higher J_C values [13, 24] come at the cost of poorer performance under strain. This work addresses that issue directly by measuring the magnetic field, temperature and strain tolerance of a PIT strand and comparing the performance to the other classes of strands listed in figure 1 [11–13, 25]. There are limited data in the literature on PIT Nb_3Sn including the strain dependence of J_C taken at 4.2 K and 12 T [26] and J_C at fixed strain as a function of field. In this paper we present detailed $J_C(B, T, \varepsilon)$ data and the associated scaling law for the PIT Nb_3Sn strand. Limited strain cycling (fatigue) tests during the measurement demonstrate that the $J_C(B, T, \varepsilon)$ data are in the reversible strain range and hence that there is no damage to the strand filaments during the measurements. The relation between n-value and critical current is also provided.

The structure of the paper is as follows. Section 2 describes the reaction and mounting procedure used in this work and an outline of the probe used to make these measurements. Section 3 provides the raw critical current density (J_C) and index of transition (n) data for the PIT strand and a comparison of equivalent data for other types of strands. In section 4, the analysis of the data is presented including the parameterization of the J_C data [27] and the n data [28, 29]. The associated fitting parameters are also provided in this section. In section 5, the properties of the PIT strand are discussed and the paper then concludes.

2. Experimental details

2.1. Samples and heat treatments

The PIT Nb_3Sn strand investigated was manufactured by Shapemetal Innovation (SMI)—the PIT technology was purchased by European Advanced Superconductors (EAS) in Dec. 2006. The wire had a diameter of 0.81 mm, a billet number B212 and 276 filaments. The wire is based on a standard (high energy physics) 288 filament ternary PIT design [10] but the inner ring of 12 filaments have been replaced by Cu in order to adjust the Cu/non Cu ratio to 1 as required for fusion applications. The hard Cr-coating thickness was ∼2.4 μm and the residual resistivity ratio (RRR) was ∼200. The extrapolated value of J_C (non-Cu) exceeded ∼2450 A mm^{-2} at 4.2 K and 12 T (equivalent to a critical current (I_C) ∼ 630 A).

The strand was heat-treated in an argon atmosphere on oxidized stainless-steel mandrels in a three-zone furnace, with an additional thermocouple positioned next to the sample in order to monitor and control the temperature. The heat-treatment schedule was: ramp up to 675 °C at 50 °C h^{-1} followed by a dwell for 50 h and then ramp down at 50 °C h^{-1}. The reaction time is much shorter than the optimal treatment for maximum J_C which has been found for (some) PIT strands to be 320 h at 625 °C [15, 25]. After reaction, the wire was etched in hydrochloric acid to remove the chrome and transferred to a nickel-plated Ti–6Al–4V helical spring [30, 31], to which it was attached by copper plating and soldering.

2.2. Apparatus and techniques

After the strand was attached to the spring, it was mounted onto our purpose-built $J_C(B, T, \varepsilon)$ probe [27, 32, 33]. The measurements were carried out in Durham in magnetic fields up to 14.5 T. For measurements at 4.2 K, the sample was in direct contact with the liquid helium. For variable-temperature measurements above 4.2 K, the probe provides a vacuum chamber around the sample and the temperature is maintained during the measurement using three sets of independently controlled Cernox thermometers and constantan wire heaters [34] distributed to produce a uniform temperature profile along the turns of the spring. To apply strain, the spring is twisted via concentric shafts attached to the spring: the inner shaft connects a worm-wheel system at the top of the probe to the top of the spring, and the outer shaft is connected to the bottom of the spring via an outer can [35].

At specified values of magnetic field, temperature and strain, measurements are made of the voltage (V) across sections of the strand as a function of a slowly-increasing

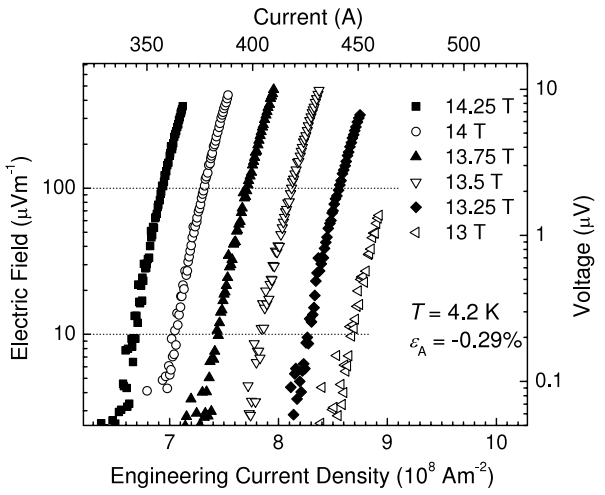

Figure 2. Log–log plot of electric field versus engineering current density (and voltage versus current) for the PIT strand at 4.2 K, with $\varepsilon_A = -0.29\%$ in magnetic fields between 13 and 14.25 T in increments of 0.25 T.

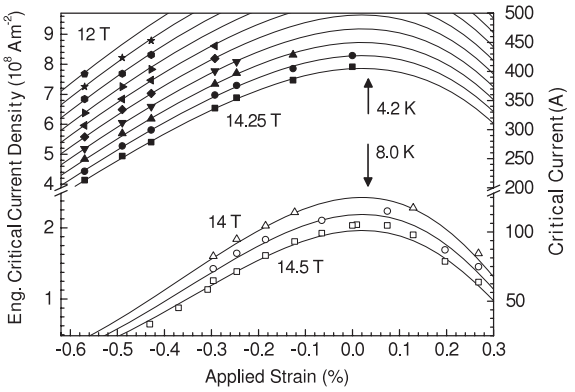

Figure 3. Engineering critical current density (and critical current) as a function of applied strain at 4.2 K in magnetic fields from 12 to 14.25 T in increments of 0.25 T and at 8 K in magnetic fields of 14, 14.25 and 14.5 T. The lines are provided by the Durham scaling law.

current through it. The voltage noise is typically a few nV, predominantly from the Johnson noise from the voltage taps [36]. The voltage across a section of the wire (typical length: ∼20 mm) was measured using a nanovolt amplifier and a digital voltmeter and the current was measured using a four-terminal standard resistor. Throughout this paper we quote an engineering critical current density J_C which is defined as the critical current (I_C) divided by the entire cross-sectional area of the wire (unless it is specified as non-Cu J_C) and is most relevant for magnet design engineers. This avoids any ambiguity with the data that can be introduced when including a nominal value for the Cu/non-Cu ratio or the area of the reacted Nb_3Sn material. The electric field (E) criterion used for J_C is 10 μV m^{-1} and the index of transition or n-value is calculated using the power-law expression $E \propto J^n$ with E in the range between 10 and 100 μV m^{-1} (see the dotted lines in figure 2). Details of the experimental apparatus and techniques have been provided previously [31, 35, 37, 38].

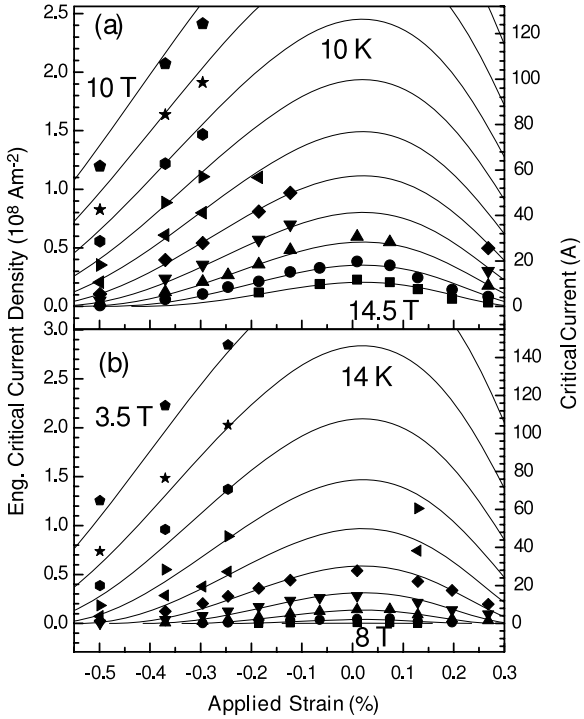

Figure 4. Engineering critical current density (and critical current) as a function of applied strain in magnetic fields (a) from 10 to 14.5 T at 10 K, and (b) from 3.5 to 8 T at 14 K. The increment in the magnetic field is 0.5 T. The lines are provided by the Durham scaling law.

3. Results

3.1. Critical current versus strain and field at variable temperature

Figure 1 shows J_C (and I_C) as a function of magnetic field at 4.2 K for the four types of strands at zero applied strain, i.e. bronze-route [27], advanced internal-tin [39], RRP [13] and PIT Nb_3Sn strands. Figure 2 shows a typical set of electric field–current density (E–J) (and voltage–current: V–I) characteristics measured at 4.2 K with the applied strain (ε_A) at −0.29% on a log–log plot for the PIT strand. Figures 3 and 4 show J_C (and I_C) of the PIT strand as a function of applied strain at 4.2, 8, 10 and 14 K in various magnetic fields. The well-known inverted quasi-parabolic behaviour for J_C as a function of applied strain is observed. Limited 12 K data were also measured (not displayed here). Figure 5 shows some reversibility data taken at 8 K under compression and tension—the irreversibility shown in this figure is associated with temperature variations of ±120 mK. The data in figures 3–5 provide strong evidence that the strand filaments have remained undamaged throughout these measurements and that the precompression in these PIT strands is small. For a direct comparison with other types of Nb_3Sn strands, the normalized critical current of the PIT strand is plotted as a function of intrinsic strain (ε_I) in figure 6 at 4.2 K when B = 14 T. By definition the intrinsic strain (ε_I) is given by $\varepsilon_I = \varepsilon_A - \varepsilon_M$, where ε_M is chosen so that ε_I is zero when J_C is a maximum [40–42]. In this figure, the symbols are from the measurements and the lines are derived from the

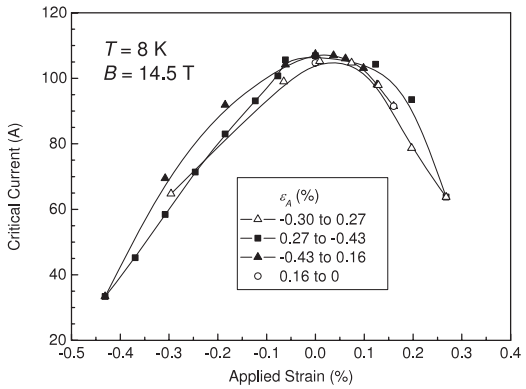

Figure 5. The critical current as a function of applied strain in 14.5 T field at $T = 8$ K, for the PIT (SMI) strand during strain cycling. The lines are guides to the eye.

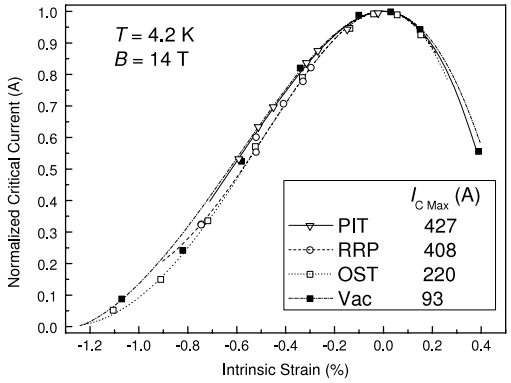

Figure 6. Normalized critical current as a function of critical current in 14 T at $T = 4.2$ K for the four types of strands. The symbols are experimental data points. The lines were calculated using the Durham scaling law.

relevant scaling laws. The peak values of the critical current are provided in figure 6—note that all these 0.81 mm strands were measured in a similar way on helical springs and that the PIT strand has the highest $I_{C\,Max}$ value. It is clear that there is no marked additional strain sensitivity for the critical current of the PIT strand compared with other types of Nb_3Sn strands.

3.2. n-value

Using the power-law expression [43–46] $E \propto J^n$, n-values for PIT strand were obtained over the technical interest range from 10 to 100 μV m^{-1} of electric field (E). The n-value and the normalized n-value of the PIT strand as a function of intrinsic strain (ε_I) are displayed in figure 7 along with other types of Nb_3Sn strands, where $T = 4.2$ K and $B = 14$ T. The n-value is significantly higher than other Nb_3Sn strands (see figure 7(a)), while the normalized n-value as a function of intrinsic strain shows quite similar behaviour (see figure 7(b)) [11]. The similar inverted quasi-parabolic behaviour [11] for the n-value, can be characterized at all temperatures and fields by plotting $n - 1$ versus the critical current as shown in figure 8 using equation (6) which will be discussed below in section 4.

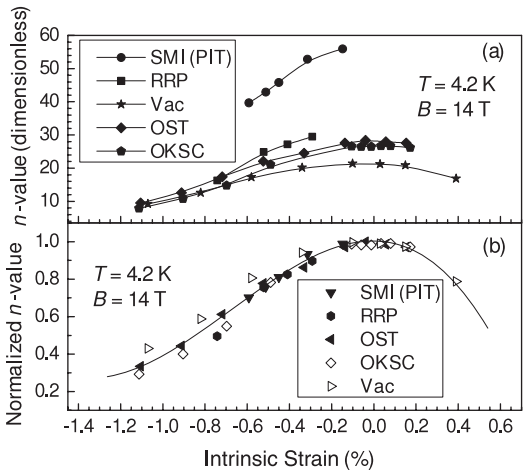

Figure 7. (a) n-value and (b) normalized n-value as a function of intrinsic strain for PIT (SMI) strand compared with other types of Nb_3Sn strands. All lines are guides to the eye.

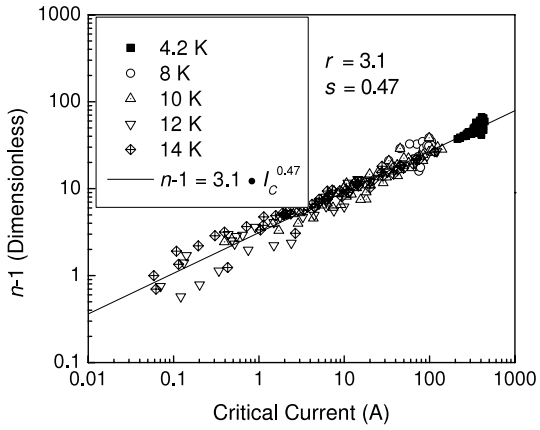

Figure 8. $n - 1$ as a function of critical current at $T = 4.2$, 8, 10, 12 and 14 K for the PIT (SMI) strands. The solid line shows a universal fit made using equation (6), where $r = 3.1$ and $s = 0.47$.

4. Analysis

4.1. Variable-strain critical current data analysed by the scaling law

The $J_C(B, T, \varepsilon)$ data at an electric field (E) of 10 μV m^{-1} are parameterized using the Durham scaling law described previously [27], which involves the following relations:

$$J_C(B, T, \varepsilon_I) = A(\varepsilon_I)[T_C^*(\varepsilon_I)(1 - t^2)]^2[B_{C2}^*(T, \varepsilon_I)]^{n-3} \times b^{p-1}(1 - b)^q \quad (1)$$

$$B_{C2}^*(T, \varepsilon_I) = B_{C2}^*(0, \varepsilon_I)(1 - t^\nu) \quad (2)$$

$$\left(\frac{A(\varepsilon_I)}{A(0)}\right)^{1/u} = \left(\frac{B_{C2}^*(0, \varepsilon_I)}{B_{C2}^*(0, 0)}\right)^{1/w} = \frac{T_C^*(\varepsilon_I)}{T_C^*(0)} \quad (3)$$

$$\frac{B_{C2}^*(0, \varepsilon_I)}{B_{C2}^*(0, 0)} = 1 + c_2\varepsilon_I^2 + c_3\varepsilon_I^3 + c_4\varepsilon_I^4, \quad (4)$$

$$\varepsilon_I = \varepsilon_A - \varepsilon_M, \quad (5)$$

where J_C is the engineering critical current density, ε_A is the applied strain, ε_I is the intrinsic strain, ε_M is the applied strain

Table 1. Scaling law parameters for the PIT (SMI) strand derived from variable magnetic field, variable temperature and variable strain, J_C data. The four parameters in bold were not varied in the fitting procedure.

p	q	$\boldsymbol{n}$	$\boldsymbol{v}$	$\boldsymbol{w}$	$\boldsymbol{u}$	ε_M (%)
1.1753	2.655	***2.500***	***1.500***	***2.200***	***0***	0.020
$A(0)$						
(A m^{-2} T^{3-n} K^{-2})	$T_C^*(0)$ (K)		$B_{C2}^*(0,0)$ (T)	c_2	c_3	c_4
1.356×10^8	17.47		29.46	−0.6153	−0.5780	−0.3002

Table 2. Proposed official ITER scaling parameters for the PIT (SMI) strand derived from variable magnetic field, variable temperature and variable strain, J_C data.

p	q	C	C_{a1}	C_{a2}
1.0	2.807	2.068×10^{11}	208.2461	189.3848
$\varepsilon_{0,a}$ (%)	ε_M (%)	$B_{C20\,max}^*(0,0)$ (T)		$T_{C0\,max}^*(0)$ (K)
0.3246	0.0274	30.93		17.03

at the peak, T_C^* is the effective critical temperature, $t = T/T_C^*$ is the reduced temperature, B_{C2}^* is the effective upper critical field and $b = B/B_{C2}^*$ is the reduced field. We have confirmed that there is little loss of accuracy parameterizing the strands if the number of free parameters is reduced to 9 and universal values of $n = 2.5$, $v = 1.5$, $w = 2.2$, $u = 0$ are used [27, 47]. The $J_C(B, T, \varepsilon)$ data set for the PIT Nb_3Sn strand presented in this paper are given in the table 1, with 9 free parameters in the parameterization process. The four parameters given in bold in table 1 were not varied in the fitting procedure. Although $T_C^*(0)$ was not fixed during the scaling process, the derived value of $T_C^*(0)$ was close to the accepted value (∼17.5 K) [27]. The precompression strain for this PIT strand is less than 0.1% ($\varepsilon_M \sim 0.02\%$) which is similar to that found for an RRP strand ($\varepsilon_M \sim 0.07\%$) also measured on an Ti-alloy helical spring [13]. We have also parameterized the whole data set using the proposed ITER scaling law [48], which gave a lower accuracy (RMS ∼ 4.1 A) compared with Durham scaling (RMS ∼ 3.2 A) as has been found before [48]. The associated 9 parameters for ITER scaling are provided in table 2.

4.2. Relationship between n-value and critical current

The n-value is usually considered as a 'quality index' that characterizes the sharpness of the E–J transition in technological superconductors and needs to be correctly parameterized for magnet design purposes [28, 29, 46, 49, 50]. In figures 6 and 7, the n-value is clearly strongly magnetic field, temperature and strain dependent [51, 52]. Although the n-value of the PIT strand is two or three times larger than other strands the normalized n-value as a function of intrinsic strain is broadly similar to the Vac, OST (internal-tin) and RRP. Smooth stable V–I characteristics have been observed with currents up to 1.8 kA in PIT strand [53]. Given the similar inverted quasi-parabolic behaviour found experimentally for both the n-value and the critical current as a function of intrinsic strain, the relation between the n values and I_C was analysed using the following well-known modified power law [11, 44]

$$n(B, T, \varepsilon_I) = 1 + r(T, \varepsilon_I)\,[I_C(B, T, \varepsilon_I)]^{s(T,\varepsilon_I)} \qquad (6)$$

where $r(T, \varepsilon_I)$ are $s(T, \varepsilon_I)$ are taken as constants at a given temperature and applied strain. Figure 8 demonstrates that to first order the $n - 1$ values are a universal function of critical current, which indicates that $s(T, \varepsilon_I)$ and $r(T, \varepsilon_I)$ only very weakly depend on the intrinsic strain and temperature and have average values of 3.1 and 0.47 respectively. Despite the high n-values for the PIT strands, the functional forms for s and r are consistent with previous work on different types of strands [11].

5. Discussion and conclusions

The high energy Physics and NMR communities are driving the demand for high performance Nb_3Sn strands with high J_C in high magnetic fields. Non-Cu J_C in PIT strands [1, 8, 14] now exceeds ∼2500 A mm^{-2} which can only otherwise be achieved in RRP [1, 8] Nb_3Sn strands. As a result of the Nb_3Sn formation inside the very uniform tin-shielding niobium tubes [9, 54] the filaments can be inherently decoupled (the 'inside-out' design also makes them magnetically transparent [55]). In this work, we have used a short heat-treatment (which is beneficial/cheaper for technological applications) yet achieved high J_C due to the rapid growth of the thick A-15 layer. The V–I transitions are very sharp characterized by the high n-values and consistent with decoupled filaments. It has been shown that the n-value of superconducting wires can be consider inversely proportional to the standard deviation of the distribution of the local critical currents in the filaments [29]. In this context, increases in n-values in PIT strands can be expected to be correlated with increases in current densities when the process for achieving high values is associated with improved filament uniformity and better compositional homogeneity.

This paper presents a detailed set of $J_C(B, T, \varepsilon)$ data which demonstrate unequivocally that the higher J_C does not come at the price of increased strain sensitivity. There are two important aspects of strain sensitivity—the intrinsic strain sensitivity of the critical current density and the strain window within which the composite strand remains broadly reversible [13]. The parameters in table 1 and the data in figure 6 demonstrate that the intrinsic properties of PIT strands are similar to other strands. Although the strain window is not investigated extensively in this work, these PIT strands can be subjected to significant tensile strain up to at least 0.25% without breaking, which is consistent with the excellent performance of the cables made out of PIT strand tested in Fermilab [56] and a reasonably large reversible strain window. The strain tolerance found here in tension is also consistent with a metallographic investigation where filament breakage

did not occur up to a bend strain of 0.5% in PIT Nb_3Sn [57]. These bending strain measurements suggest that the intrinsic transverse strain tolerance of PIT strains may also be similar to other types of strands although further work is required to confirm this. We note that we did not test these strands to destruction. Hence this work demonstrates that the reversible strain window at least encompasses $-0.60\% < \varepsilon_I < 0.25\%$ but does not characterize the full extent of the reversible strain window.

The raw $J_C(B, T, \varepsilon)$ data for PIT strand together with n-values and Durham scaling law parameterizations are available at http://www.dur.ac.uk/superconductivity.durham. In terms of the large critical currents and n-values, short heat-treatment schedule, and the conventional strain sensitivity reported in this paper, the PIT strand investigated clearly has very significant technological value if the cost of fabrication can be reduced and significant academic value as an excellent system to evaluate the ultimate potential of polycrystalline Nb_3Sn strands.

Acknowledgments

The authors acknowledge the help and support of J Orr, S Pragnell, M Raine and A Vostner. We also acknowledge the many discussions about critical current we have had with those in the community including: D Bessette, D Bruzzone, N Cheggour, J Duchateau, J Ekin, W H Fietz, H Fillunger, B Karlemo, P Komarek, R Maix, N Martovetsky, N Mitchell, J Minervini, A Nyilas, A Nijhuis, A Portone, K Osamura, E Salpietro, L Savoldi Richard, J Schultz and R Zanino.

References

[1] Vostner A and Salpietro E 2006 *Supercond. Sci. Technol.* **19** S90–5
[2] Zanino R, Mitchell N and Savoldi-Richard L 2003 *Cryogenics* **43** 179–97
[3] Zanino R and Savoldi-Richard L 2003 *Cryogenics* **43** 79–90
[4] Mitchell N 2003 *Fusion Eng. Des.* **66–8** 971–93
[5] Wada H and Kiyoshi T 2002 *IEEE Trans. Appl. Supercond.* **12** 715–7
[6] Devred A *et al* 2006 *Supercond. Sci. Technol.* **19** S67–83
[7] Farinon S, Boutboul T, Devred A, Fabbricatore P, Leroy D and Oberli L 2007 *IEEE Trans. Appl. Supercond.* **17** 1136–9
[8] Hong S, Field M B, Parrell J A and Zhang Y Z 2006 *IEEE Trans. Appl. Supercond.* **16** 1146–51
[9] Lindenhovius J L H, Hornsveld E M, den Ouden A, Wessel W A J and ten Kate H H J 2000 *IEEE Trans. Appl. Supercond.* **10** 975–8
[10] Godeke A, den Ouden A, Nijhuis A and ten Kate H H J 2008 *Cryogenics* **48** 308–16
[11] Taylor D M J and Hampshire D P 2005 *Supercond. Sci. Technol.* **18** 297–302
[12] Hampshire D P, Taylor D M J, Foley P and Keys S A 2001 *University of Durham Report No. DurSC0601*
[13] Lu X F, Pragnell S and Hampshire D P 2007 *Appl. Phys. Lett.* **91** 132512
[14] Michiel M D and Scheuerlein C 2007 *Supercond. Sci. Technol.* **20** L55–8
[15] Boutboul T, Oberli L, den Ouden A, Pedrini D, Seeber B and Volpini G 2009 *IEEE Trans. Appl. Supercond.* **19** 2564–7
[16] Lee P J and Larbalestier D C 2001 *IEEE Trans. Appl. Supercond.* **11** 3671–4
[17] Flukiger R, Uglietti D, Senatore C and Buta F 2008 *Cryogenics* **48** 293–307
[18] Hampshire D P 1998 *Physica* C **296** 153–66
[19] Sneary A B, Friend C M, Vallier J C and Hampshire D P 1999 *IEEE Trans. Appl. Supercond.* **9** 2585–8
[20] Osamura K, Nonaka S, Matsui M, Oku T, Ochiai S and Hampshire D P 1996 *J. Appl. Phys.* **79** 7877–83
[21] Flukiger R, Hossain M S A and Senatore C 2009 *Supercond. Sci. Technol.* **22** 085002
[22] Gregory E, Zeitlin B A, Tomsic M, Peng X, Sumption M D and Collings E W 2007 *IEEE Trans. Appl. Supercond.* **17** 2664–7
[23] Bruzzone P *et al* 2007 *IEEE Trans. Appl. Supercond.* **17** 1370
[24] Nijhuis A, Ilyin Y and Abbas W 2008 *Supercond. Sci. Technol.* **21** 065001
[25] Lu X F and Hampshire D P 2009 *IEEE Trans. Appl. Supercond.* **19** 2619–23
[26] Nijhuis A, Ilyin Y, Wessel W A J and Abbas W 2006 *Supercond. Sci. Technol.* **19** 1136–45
[27] Taylor D M J and Hampshire D P 2005 *Supercond. Sci. Technol.* **18** S241–52
[28] Warnes W H and Larbalestier D C 1986 *Cryogenics* **26** 643–53
[29] Hampshire D P and Jones H 1987 *Cryogenics* **27** 608–16
[30] Walters C R, Davidson I M and Tuck G E 1986 *Cryogenics* **26** 406–12
[31] Taylor D M J and Hampshire D P 2005 *Supercond. Sci. Technol.* **18** 356–68
[32] Cheggour N and Hampshire D P 1999 *J. Appl. Phys.* **86** 552–5
[33] Keys S A and Hampshire D P 2003 *Supercond. Sci. Technol.* **16** 1097–108
[34] Brandt B L, Liu D W and Rubin L G 1999 *Rev. Sci. Instrum.* **70** 104–10
[35] Cheggour N and Hampshire D P 2000 *Rev. Sci. Instrum.* **71** 4521–30
[36] Higgins J S and Hampshire D P 2009 in progress
[37] Keys S A, Koizumi N and Hampshire D P 2002 *Supercond. Sci. Technol.* **15** 991–1010
[38] Keys S A and Hampshire D P 2003 *Handbook of Superconducting Materials* ed D Cardwell and D Ginley (Bristol: Institute of Physics Publishing) pp 1297–322
[39] Lu X F, Taylor D M J and Hampshire D P 2008 *Supercond. Sci. Technol.* **21** 105016
[40] Luhman T, Suenaga M and Klamut C J 1978 *Adv. Cryog. Eng.* **24** 325–30
[41] Rupp G 1977 *IEEE Trans. Appl. Supercond.* **13** 1565–7
[42] Markiewicz W D 2004 *Cryogenics* **44** 895–908
[43] Volker F 1970 *Part. Accel.* **1** 205
[44] Taylor D M J, Keys S A and Hampshire D P 2002 *Physica* C **372** 1291–4
[45] Taylor D M J, Foley P, Niu H and Hampshire D P 2004 *Durham University Report No. EFDA/03-1103*
[46] Bruzzone P 2004 *Physica* C **401** 7–14
[47] Corato V, Muzzi L, della Corte A and Viola R 2009 *Fusion Eng. Des.* **84** 623–7
[48] Bottura L and Bordini B 2008 *IEEE Trans. Appl. Supercond.* **19** 1521–4
[49] Ghosh A K 2004 *Physica* C **401** 15–21
[50] Hampshire D P and Jones H 1985 *Magn. Technol.* **9** 531–5
[51] Mitchell N 2004 *Physica* C **401** 28–39
[52] Martovetsky M 2004 *Physica* C **401** 22–7
[53] Barzi E, Andreev N, Bordini B, Del Frate L, Kashikhin V V, Turrioni D, Yamada R and Zlobin A V 2005 *IEEE Trans. Appl. Supercond.* **15** 3364–7
[54] Cooley L D, Fischer C M, Lee P J and Larbalestier D C 2004 *J. Appl. Phys.* **96** 2122–30
[55] Hawes C D, Lee P J and Larbalestier D C 2000 *IEEE Trans. Appl. Supercond.* **10** 988–91
[56] Feher S *et al* 2005 *IEEE Trans. Appl. Supercond.* **15** 1550–3
[57] Jewell M C, Lee P J and Larbalestier D C 2003 *Supercond. Sci. Technol.* **16** 1005–11